RI 8594

Bureau of Mines Report of Investigations/1982

Electromagnetic Radiation From Rock Failure

By David R. Hanson and Glen A. Rowell

UNITED STATES DEPARTMENT OF THE INTERIOR

Report of Investigations 8594

Electromagnetic Radiation From Rock Failure

By David R. Hanson and Glen A. Rowell

UNITED STATES DEPARTMENT OF THE INTERIOR
James G. Watt, Secretary
BUREAU OF MINES
Robert C. Horton, Director

This publication has been cataloged as follows:

Hanson, David R

Electromagnetic radiation from rock failure.

(Report of investigations ; 8594)

Bibliography: p. 21.

Supt. of Docs. no.: I 28.23:8594.

1. Rocks—Electric properties. 2. Electromagnetic waves. 3. Rock mechanics. I. Rowell, Glen A. II. Title. III. Series: Report of investigations (United States. Bureau of Mines) ; 8594.

TN23.U43 [QE431.6.E4] 622s [622'.8] 81-607312 AACR2

CONTENTS

ILLUSTRATIONS

ILLUSTRATIONS--Continued

TABLE

ELECTROMAGNETIC RADIATION FROM ROCK FAILURE

by

David R. Hanson[1] and Glen A. Rowell[2]

ABSTRACT

Experimental work performed by the Bureau of Mines in a laboratory environment has shown that the formation of failure zones within certain rock types is accompanied by the emission of significant amounts of radiofrequency (RF) electromagnetic (EM) energy. This radiation was detected using nonresonant, "electrically short," broad-band antennas. Rock types for which emission was observed include granite, quartzite, and taconite; sandstone and marble did not emit measurable radiation. Amplitude spectra of the radiation showed the energy to be concentrated between 10 and 40 kilohertz. These data indicate that emission is directional, but this has not yet been proven. In addition, amplitude of RF emission increases with increasing crack size. Since emission was observed only for brittle quartz-bearing rocks, it appears the formation of piezoelectric fields is a necessary condition for RF radiation. Plausible mechanisms for emission include rapid decay of piezoelectric fields accompanying the sudden stress release at failure and/or the acceleration of an "exoelectron plasma" through the intense local piezoelectric fields.

Since emission appears to increase with the scale of failure, and since antennas do not need to be coupled directly to rock surfaces as with conventional geophones, the possibility of developing a portable system to monitor seismically active areas exists.

INTRODUCTION

One of the objectives of rock failure investigations performed at the Bureau of Mines is to relate the anomalous activity of rocks before and during failures on a laboratory scale to activity present in rock bursts. This anomalous activity has previously included tilts, seismicity, radon emission,

[1]Mining engineer.
[2]Mechanical engineer.
Both authors are with the Denver Research Center, Bureau of Mines, Denver, Colo.

and V_p/V_s ratios[3] (1-6,14).[4] Recently, another anomalous activity has been observed to accompany the failure of certain laboratory specimens, that is, the emission of radiofrequency (RF) electromagnetic (EM) energy.

Although the formation of anomalous electric and magnetic fields has been predicted by some theories of failure (2-5,14, 16), and in some cases observed in the field (7, 16), detailed investigation of these phenomena under controlled conditions is only beginning. In her book on electrification phenomena in rocks, Parkhomenko (16) mentions that fragmentation of LiF and NaCl crystals gives rise to bursts of both visible and nonvisible electromagnetic radiation but presents no quantitative results. More recently, Vorobev, (17) scratched a series of dielectric materials (LiF, KCl, NaCl, quartz, feldspar, fluorite, and talc) with a diamond pyramid and observed pulsed radiofrequency emission. In this work the intensity of radiation was found to increase to a saturation level as load on the pyramid and hardness of the sample increased.

Nitsan (15) has recently performed work in which he stressed samples of piezoelectric rocks in uniaxial compression, by pressing a steel ball against a flat surface, and by crushing irregular samples in a vise. Using a ferrite core AM radio coil and amplifier, Nitsan observed exponentially decaying bursts of electromagnetic energy in the 1- to 10-megahertz frequency range accompanying failure. For all quartz-bearing rocks tested (granite, granodiorite, sandstone, and quartzite) RF signals were detected, while for nonpiezoelectric materials (basalt, obsidian, limestone, aluminum, steel, glass, and plastic) no signals were observed. These results led Nitsan to propose that the probable mechanism for emission was the rapid decay of the piezoelectric field that results from the sudden stress release as the sample fractures. He further proposed that the frequency content of the signal would be directly proportional to the rate of stress release and hence inversely proportional to the grain size of the rock. Results presented by Nitsan support this hypothesis as the spectra of bursts seen in his work shifted to higher frequencies as grain size decreased.

Work performed at the Bureau of Mines and described in this paper shows that the emission of electromagnetic energy also exists in the 10- to 200-kilohertz range. A series of specimens of granite, quartzite, taconite, sandstone, and marble were tested for electromagnetic radiation as they were failed under uniaxial compression. In addition to an array of three antennas, load, two orthogonal moments, acceleration, and acoustic emission were monitored in an attempt to relate EM radiation to other indicators of failure.

ACKNOWLEDGMENTS

The authors wish to express their gratitude to Professors George V. Keller, Maurice W. Major, and Fun-Den Wang of the Colorado School of Mines, Golden, Colorado, and to Brian T. Brady and Verne E. Hooker of the U.S. Bureau of Mines for their consultation during the experiments performed in this work.

---

[3] V_p refers to compressional wave velocity and V_s to shear wave velocity.

[4] Underlined numbers in parentheses refer to items in the list of references at the end of this report.

EXPERIMENTAL PROCEDURE

NX-size (55-millimeter diameter) cores of Red Texas Granite, Barre Granite, Dakota Sandstone, Carthage Marble, and quartzite from the Galena Mine, Wallace, Idaho, were cut and ground to a final length of 135 millimeters for use in uniaxial compression tests. In addition, a number of smaller samples (38-millimeter diameter, 95-millimeter length) of Mather Iron Ore from the Marquette district of Michigan were prepared. All specimens were tested to failure in uniaxial compression in a servocontrolled materials testing system (MTS Systems Corp., 2.7 x 10^6-newton capacity).[5] Displacement rates for all tests were held at 5 x 10^{-6} meter per second (fig. 1).

The load cell used to instrument the tests allowed monitoring of axial load (F_z), and two orthogonal moments (M_x and M_y) through an array of strain gages mounted on a steel platen. Resolution of load changes with this cell is approximately 500 newtons, although noise encountered when recording data on an analog tape deck reduces the effective resolution to about 5 kilonewtons. Resonant frequencies exist at 20 kilohertz for the load and 12 kilohertz for the moments.

An Endevco model 2219E accelerometer and a Dunegan/Endevco model D9201 acoustic emission transducer (AET) were coupled to the base plate of the press to monitor acoustic signals transmitted through the specimen and press. Both were coupled to the press by means of a coupling gel (Sperry Multipurpose Ultrasonic Couplant, heavy viscosity, #50A4084). The AET has an optimum operating frequency range of 100 kilohertz to 1 megahertz. Maximum response of 1 millivolt per pascal occurs at 200 kilohertz. The accelerometer has a peak response of 380 millivolts per gravity with a 100 picofarad load. Response is essentially flat from 100 hertz to 4 kilohertz with a resonant peak at 16 kilohertz. Outputs from both the AET and the accelerometer were directed through a 20-decibel-gain amplifier before being recorded.

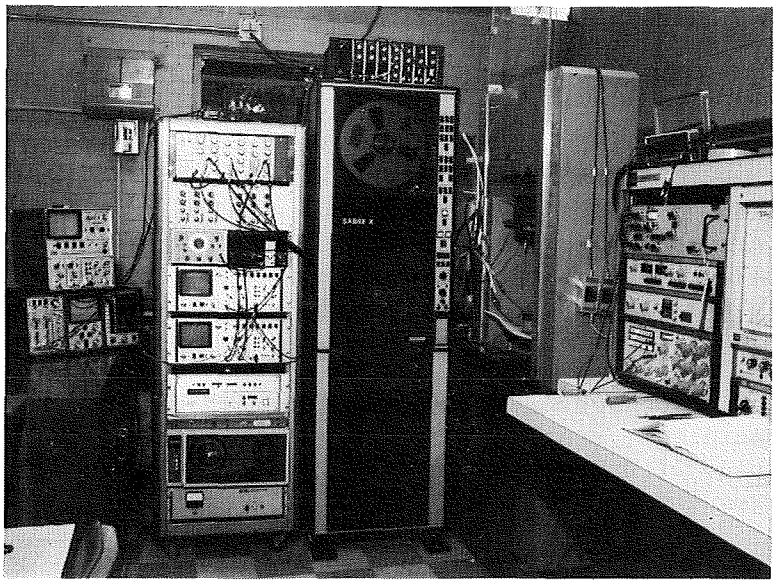

FIGURE 1. - Laboratory setup.

A single piezoelectric polymer transducer (PPT) was placed directly on the sample surface and was held in place by an elastic rubber

[5]Reference to specific trade names is made for identification only and does not imply endorsement by the Bureau of Mines.

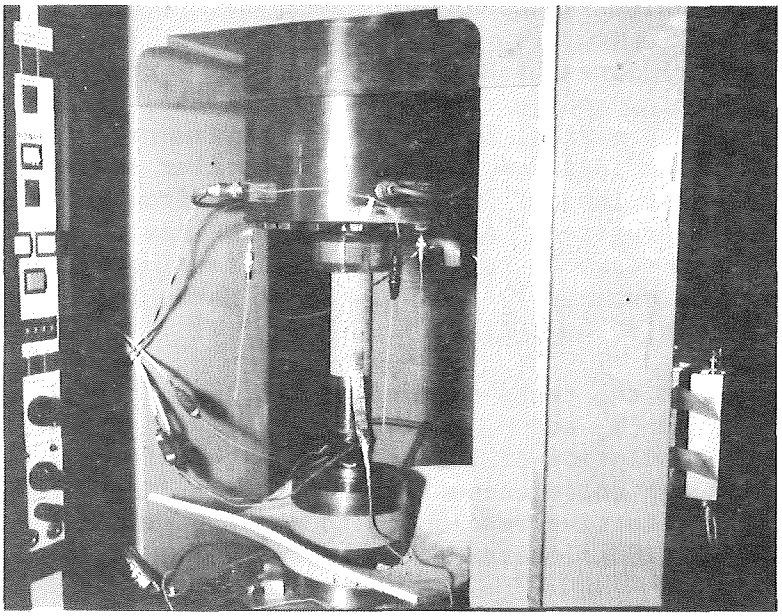

FIGURE 2. - Typical instrumentation of rock samples showing position and orientation of piezoelectric polymer transducer (PPT) and antenna.

sleeve placed over the entire sample (figs. 2-3). The PPT also serves to detect acoustic emission by creating a voltage in response to pressure waves of elastic displacements originating within the sample. However, data from the PPT added nothing to that available from the accelerometer and AET and so are not included in the figures.

The electromagnetic radiation detection devices consisted of three electrically short monopole antennas. These were constructed from a piece of 18-gage insulated wire soldered to the center conductor of a coaxial cable. Length of each dipole was 152.5 millimeters (6 inches), corresponding to a quarter wavelength of a 492-megahertz electromagnetic wave (in air). The radio frequency signals emitted from the sample and detected with the monopole antennas were input to a 40-decibel-gain preamplifier (0.5 hertz to 200 kilohertz, down 12 decibels at 1 megahertz). The signal was then bandpass-filtered from 10 kilohertz to 400 kilohertz to remove lower frequency environmental noise encountered in the laboratory. Finally, another 20 decibels of gain was applied before inputting the signal to the tape deck. The three antennas were arrayed around the specimen at 120° intervals about 120 millimeters from the surface of the rock (all three antenna axes parallel to the axis of the specimen) in an attempt to obtain information on the location of the crack within the specimen (figs. 2-3). However, time resolution obtainable with present equipment make anything more than a very rough estimate of crack location impossible.

Data from all these monitoring devices were recorded on an analog Sangamo/Schlumberger Sabre X magnetic tape deck. For these tests all recording was done in the FM mode at a speed of 6.1 meters per second (240 inches per second), which allowed a frequency range of DC to 160 kilohertz to be recorded.

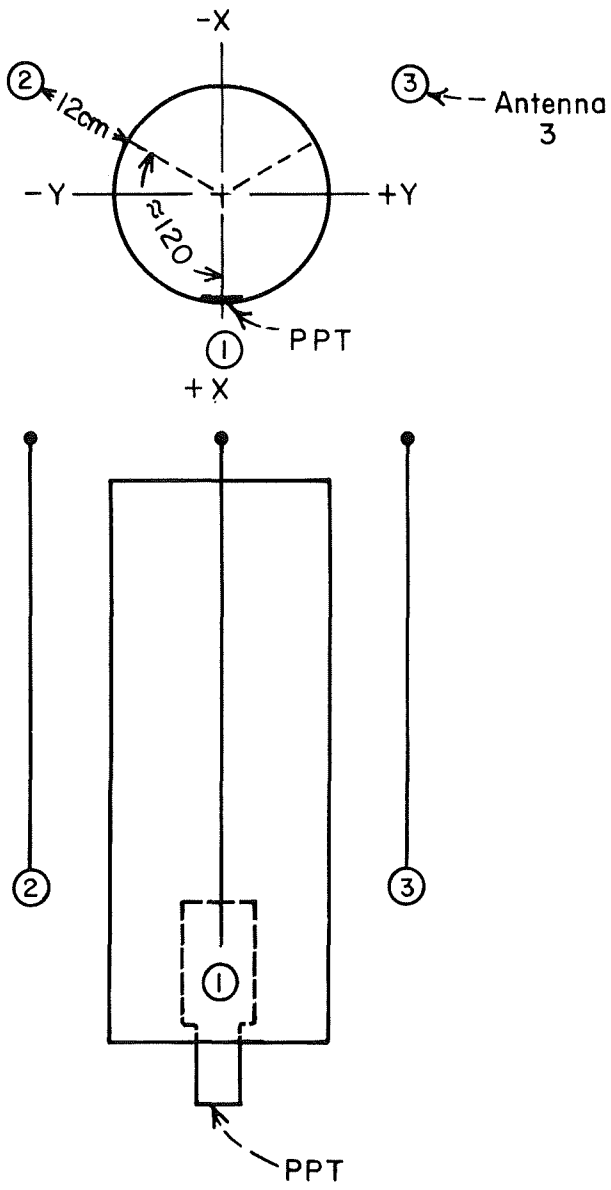

FIGURE 3. - Schematic of rock samples showing position of antennas and PPT. Letters +X, -X, +Y, -Y refer to orientation and direction of X- and Y-axes for moments.

When working with multiple data tracks it is desirable to know the absolute time differences between the same events detected by different transducers. Unfortunately, the time differences observed upon playback of the data are not only a function of the different occurrence times of the events, but also a function of misalinement between recording and playback heads. For example, if one signal is input simultaneously to two channels, when played back, there should be no time shift between the two signals. However, there is inevitably skew present between record and playback heads. The time shift caused by this skew was measured for each channel pair and the data were adjusted in time to remove this skew from the results presented in the figures. This time adjustment ranged from 0.07 to 2.56 microseconds.

In addition to time shifts due to head misalinement, shifts are present between antenna signals and all other data due to the different speed of propagation of the signals (acoustic versus speed of light). This shift causes all other signals to appear shifted later in time than the antennas. If an exact location of the event within the specimen were available, the time required for the information to travel to the transducers could be computed and removed from plots. This would then theoretically bring the plots into time coincidence since all signals would be referenced to their time of occurrence rather than their time of detection. The EM waves are assumed to arrive nearly instantaneously since they travel at the speed of light.

An exact location of events within the specimen was not available, so time adjustments were based on the assumption that events occurred near the middle of the sample. This gives a travel path in the rock for the acoustic signals of 65 millimeters (49 millimeters for iron ore). The accelerometer and AET were coupled to the base platen of the press, a distance of approximately 330 millimeters from the sample. Strain gages used to monitor the load and moments were mounted on a steel platen approximately 102 millimeters from the sample. These are the travel paths used to compute time delays in data due to acoustic (versus electromagnetic) speed of propagation. Velocities of sound in the various sample types were measured to be

	Velocity, meters per second
Steel.....	5,486
Red Texas and Barre Granite.	3,810
Mather Iron Ore.....	5,273
Carthage Marble.....	5,060
Dakota Sandstone.....	2,438
Galena Quartzite.....	5,334

Combining time delays due to velocity differences with shifts due to head misalinement gives the total time delays shown in table 1. These time delays were subtracted from figures 4-30. All data were referenced to channel 3 of the tape deck (antenna 2).

TABLE 1. - Time delay chart for the various samples

Channel	Device	Delay time, microseconds			
		Granite	Iron Ore	Quartzite Marble	Sandstone
1	Antenna 1....	0.26	0.26	0.26	0.26
3	Antenna 2....	0	0	0	0
5	Antenna 3....	.07	.07	.07	.07
7	AET.....	77.4	76.4	72.4	86.4
8	Accelerometer	79.8	78.8	74.8	88.8
10	Load.....	37.7	29.7	32.7	46.7
12	M_x.....	38.1	30.1	33.1	47.1
14	M_y.....	37.6	29.6	32.6	46.6

RESULTS

Galena Quartzite

Galena Quartzite is a fine-grained, light gray quartzite occasionally banded with veins of quartz, pyrite, galena, siderite, and tetrahedrite. It is the country rock from the Galena Mine, Wallace, Idaho. Samples were prepared from cores obtained from the drilling of holes for geophone mountings on the 4,000-foot level of the mine. Care was taken to select samples for testing which were free from obvious fractures and veining.

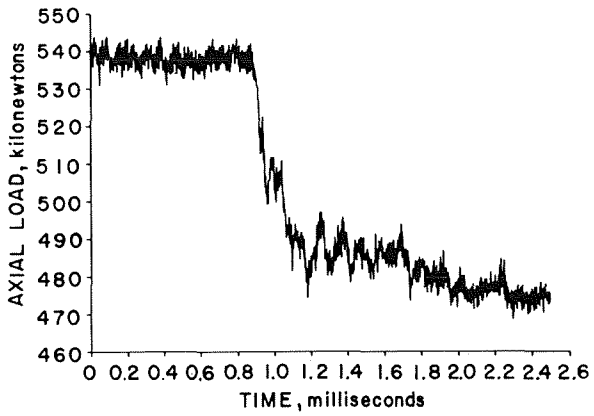

FIGURE 4. - Axial load for a preliminary failure of Galena Quartzite. Load drop began at 0.90 millisecond and totaled approximately 47 kilonewtons. Final failure occurred approximately 1 second later and involved a load drop of over 400 kilonewtons.

Devices used to monitor the tests on Galena Quartzite were an accelerometer, an AET, a load cell, and three antennas. The failure event examined for Galena Quartzite in figures 4 through 12 is one of a number of preliminary fractures that occurred about a second before catastrophic failure and is associated with a load drop of 47 kilonewtons. The final failure of the sample involved a load drop of over 400 kilonewtons, a stress drop of 170 megapascals.

Fracture onset is assumed to coincide in time with the rapid load drop and the onset of violent changes in both components of moment as seen in figures 4, 5, and 6 at 0.90 milliseconds. Moment changes can be interpreted as shifts of the load-bearing axis toward more competent rock as the sample fails. This, in turn, can be used to interpret the direction of growth of a fracture. Since a left-handed coordinate system was used, an increase in the X-moment indicates a shift of load in the +Y-direction, and an increase in Y-moment corresponds to a shift of the load-bearing axis toward the -X-direction. The orientation of axes and antennas is shown in figure 3. The magnitude of changes in M_y in figure 6 are much larger than those in M_x and so most of the sample's tilt occurred about the Y-axis. From these moments it can be inferred that the crack grew from the +X-direction to the -X-direction, or vice versa. It should also be noted that the recovery of load at 0.97 millisecond of figure 4 corresponds to a sudden moment reversal or shift of the load-bearing axis back toward the center of the sample. This

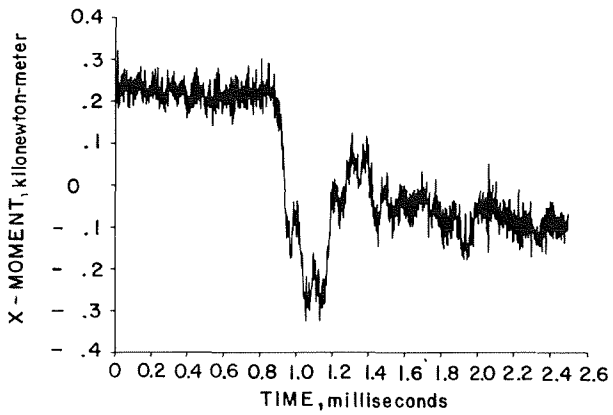

FIGURE 5. - X-component of moment for Galena Quartzite. Decreasing moment indicates movement of load-bearing axis toward the -Y-direction and vice versa. The rapid decrease in moment at 0.89 millisecond corresponds to the inception of failure in figure 4.

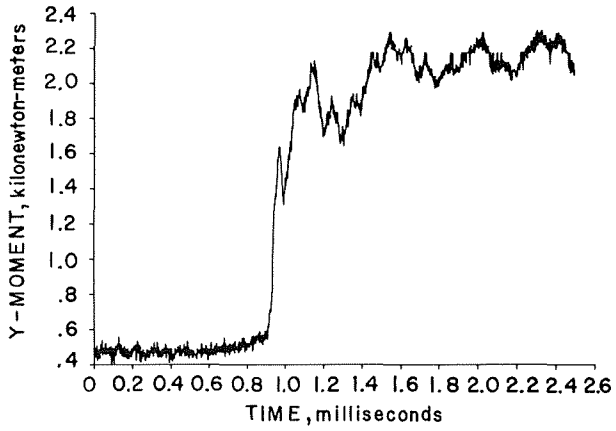

FIGURE 6. - Y-component of moment for a preliminary fracture of Galena Quartzite. Increasing moment indicates movement of the load-bearing axis toward the -X-direction and vice versa.

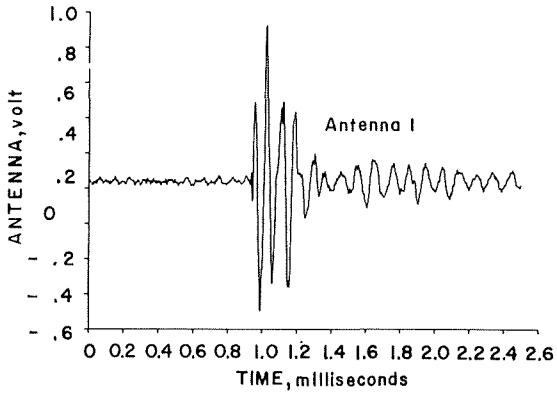

FIGURE 7. - Response of antenna to a minor crack in Galena Quartzite. Signal begins at approximately 0.90 millisecond and obtains a maximum peak-to-peak amplitude of 1.6 volt.

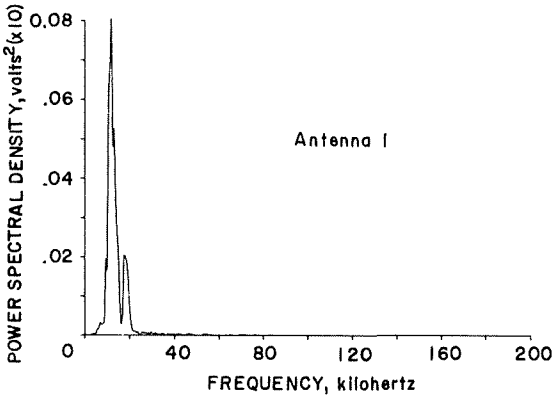

FIGURE 8. - Amplitude spectra of the antenna signal of figure 7 showing the very sharply peaked spectra at 12 kilohertz.

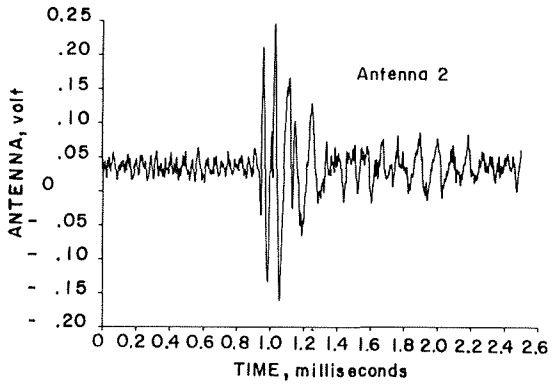

FIGURE 9. - Antenna 2 response from Galena Quartzite. Response begins at about 0.90 millisecond, but has only 0.4-volt peak-to-peak amplitude.

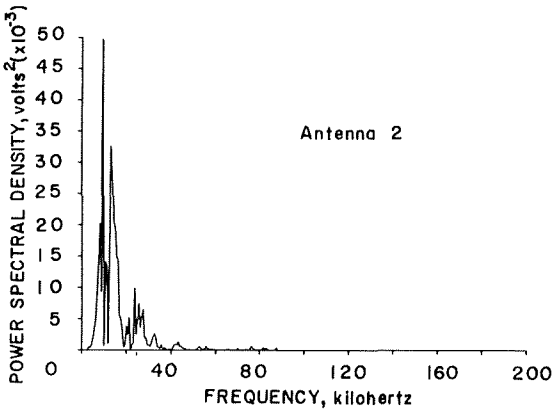

FIGURE 10. - Spectra of antenna 2. Spectral peaks occur at 8, 9.5, and 13 kilohertz.

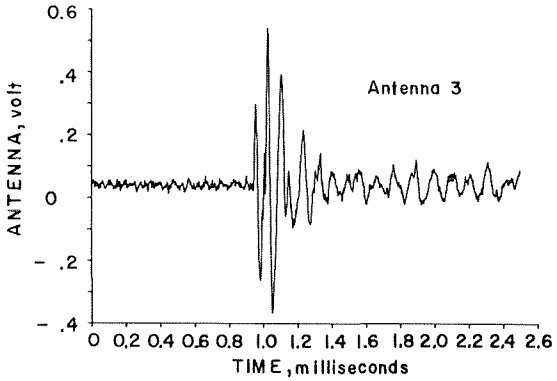

FIGURE 11. - Response of antenna 3 to Galena Quartzite. Signal arrives at about 0.95 millisecond and has a maximum peak-to-peak amplitude of 0.9 volt.

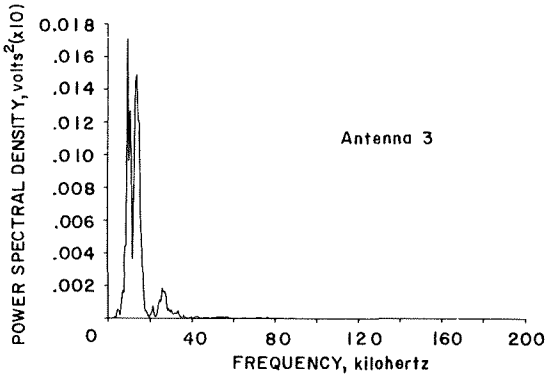

FIGURE 12. - Spectra of antenna 3. As with antennas 1 and 2, emission is sharply peaked below 20 kilohertz with peaks at 9, 10.5, and 14 kilohertz.

type of behavior was seen in all tests and can be interpreted as a reversal of dilatancy and crack closure as the steel platens advance on the sample. This will momentarily increase the competency of the rock as the cracks close and friction takes effect. Before fracture, the loading axis is nearly in the center of the sample (zero moments). As the sample fails, it violently shifts its load-bearing axis in the direction of more competent rock, with some reversals. It should be noted that the moment shifts seen in figures 5 and 6 are not due to final castastrophic failure, but rather to a minor cracking event occurring relatively early in the failure history of the sample.

All three antennas arrayed around the sample showed bursts of electromagnetic energy arriving at between 0.90 and 0.92 millisecond (figs. 7, 9, and 11). These times are slightly late compared with acoustic indicators of failure, but this is probably due to the uncertainty of the acoustic location of failure events. That is, this fracture may have been closer to the load cell than the 65 millimeters assumed to compute average time shifts. This could add as much as 12 microseconds to load and moment times. Also, if the velocity of acoustical signals through the failing quartzite differed from the 5,334 meters per second used, additional unknown time shifts could be introduced.

The important point to note, however, is the production of a burst of radiofrequency electromagnetic radiation within 50 microseconds of the formation of a failure within the rock. The failure zone giving rise to the RF pulse may not necessarily be associated with the final failure of the sample.

While the amplifier, filter, and recording system used had a rated bandwidth of 10 to 160 kilohertz, spectra of the EM signals (figs. 8, 10, and 12) peaked sharply below 40 kilohertz. This is generally the case for all tests, grain sizes, and rock types, as will be shown in subsequent tests.

Analysis of figures 7, 9, and 11 shows a rather large difference in amplitude (peak-to-peak) of the responses of the three antennas. Antenna 1 has a maximum peak-to-peak amplitude of 1.6 volts; antenna 2, 0.4 volt; and antenna 3, 0.9 volt after 60 decibel amplification and 10- to 400 kilohertz bandpass filtering. Three explanations for these differences present themselves. The first is that the crack was closest to antenna 1, and the farther the antenna from the crack, the lower the antenna response. The maximum difference in travel path between antennas 1 and 2 is about 5 centimeters. That this distance would cause a fourfold decrease in amplitude seems unlikely unless perhaps the signal is severely attenuated by having to travel through the rock (15).

However, this is unlikely. Using the formula for skin depth (13)

$$\delta = \left[\frac{2\rho}{\mu\omega} \right]^{1/2} = \left[\frac{\rho}{\pi f \mu} \right]^{1/2}$$

and assuming for granite

ρ = resistivity = 10^{-5} ohm-meters (11),

$\mu = \mu_o$ = permeability of free space

$= 4\pi \times 10^{-7}$ ohm-seconds per meter,

ω = angular frequency = $2\pi f$ radians per second,

and f = 20 kilohertz,

the skin depth is found to be 1,125 meters. This is the distance at which the amplitude of the electromagnetic signal decays by 1/e of its original value. For a distance of 5 centimeters, the attenuation of an electromagnetic wave due to this effect amounts to only 0.001 percent of its original value. It would seem, therefore, that traveling through 5 centimeters of rock could not account for the 4-to-1 amplitude variations observed. A second explanation for the observed amplitude variations is that the radiated energy from the fracture is strongly controlled by refraction of the EM wave at the rock-air interface. For a source within the rock at any position other than along the axis of the sample, refraction will occur at the boundary. It is possible the antennas lie within a "shadow zone" created by ray refraction. However, the extent to which rays of the relatively low frequency radiation observed (where conduction current dominates dielectric current) are affected is not clear.

A third possible explanation, and the one preferred by the authors, is that emission displays some degree of directionality. As mentioned earlier, analysis of the moments (figs. 5 and 6) suggests that the crack causing these events grew from the +X- to the -X-direction, or vice versa (fig. 3). Examination of the amplitude responses of the three antennas reveals that antenna 1 had the largest response. If emission is indeed directional, this could be an indication that maximum radiation is produced colinearly with crack growth. Although this type of amplitude behavior was observed in other tests, data are insufficient at this time to confirm this interpretation.

Results of this test show the production of a burst of EM energy accompanying the formation of a failure zone within the rock. In addition, the frequency content of these signals is concentrated below 40 kilohertz. Finally, the different amplitudes of the three antenna responses suggest a degree of directionality.

Red Texas Granite

Red Texas Granite is a pink, biotite fluorite granite. It is a coarse-grained, hypidiomorphic granular rock. Hoenig (9) submitted this rock for analysis and found its constituents to be microcline, 30 percent; quartz, 30 percent; plagioclase, 20 percent; biotite 20 percent; and interstitial fluorite, ≤1 percent. There were traces of magnetite, apatite, and zircon, and overall alteration was termed moderate.

Because of the large grain size of Red Texas Granite, failure of the rock in the uniaxial mode consists of a large number of preliminary cracks which gradually reduce the competency of the rock until final failure occurs. This behavior prevents the ultimate failure of the sample from being as violent or having as large a load drop as finer grained materials. Figures 13 through 23 are the results from one of the preliminary fractures which occurred a relatively long time before catastrophic failure. No indication of any load or moment changes are observable above the noise level in figures 13, 14, or 15. Load is nearly constant at 362 kilonewtons and M_x and M_y are constant at 0.22 and 0.17 kilonewton-meters respectively. The noise on these figures is due to analog tape noise.

Even though the load cell did not sense any significant changes, all other devices responded to a failure event. The accelerometer (fig. 16) begins responding at about 1.0 millisecond and continues ringing at its resonant frequency (fig. 17) throughout the remainder of the trace. As with the Galena Quartzite, all three antennas (figs. 18-23) show a very sharp, short-duration burst of electromagnetic energy commencing at about 0.96 millisecond. This response time is earlier than the accelerometer response, but this again may be due to uncertainty of the acoustic location of the event within the sample. The important points of the antenna responses are their short duration (about 200 microseconds), differing amplitudes, and sharply peaked spectra. If the antennas were excited by the voltages created by the accelerometer, they should continue responding for longer than 200 microseconds, following the waveform of the other device, which they do not. As with the Galena Quartzite, different antennas show different amplitude responses. Although slightly less peaked than the spectra of Galena Quartzite, antenna spectra for this event still peak below 40 kilohertz. Some of the frequency content in the power spectra is due to noise associated with the analog tape deck.

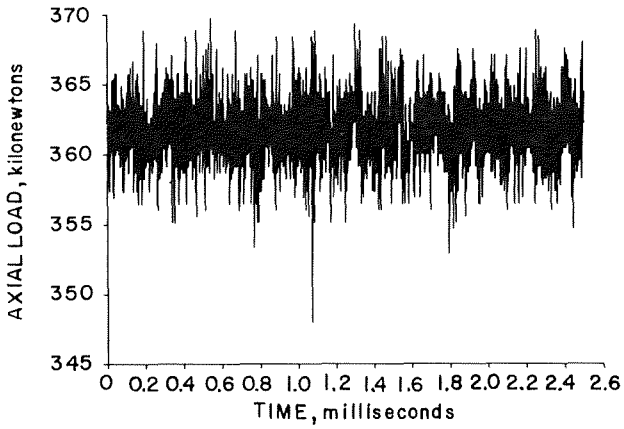

FIGURE 13. - Axial load during a preliminary fracture of Red Texas Granite sample. Note the constant load of 362 kilonewtons with no indication of a load drop. Fuzz on the trace is due to analog tape noise.

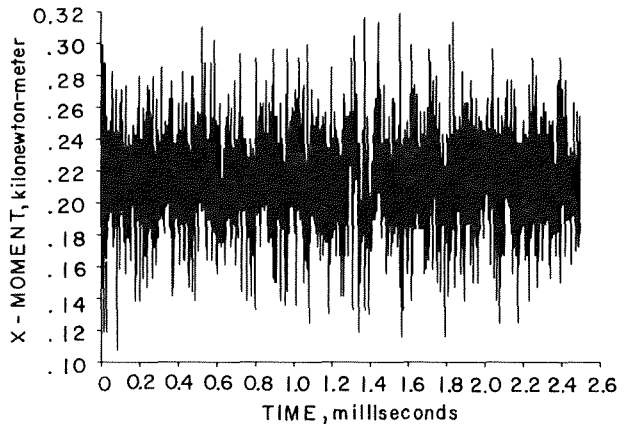

FIGURE 14. - X-component of moment, Red Texas Granite. There is no indication of any changes indicative of failure.

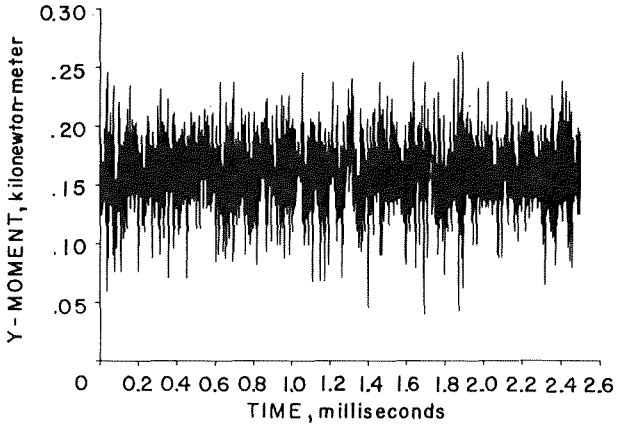

FIGURE 15. - Y-component of moment, Red Texas Granite. Again there is no change from the constant value of 0.17 kilonewton-meter other than an analog tape noise.

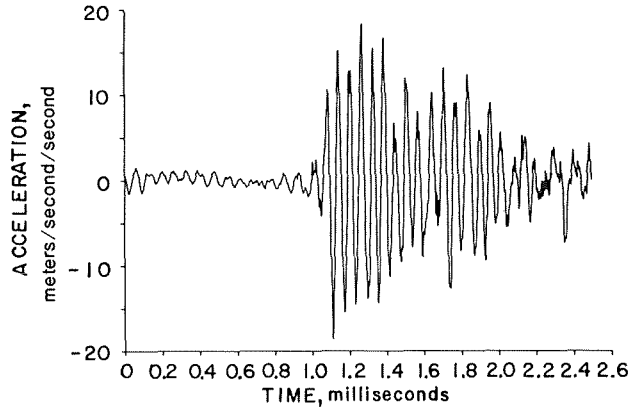

FIGURE 16. - Acceleration of the base plate of the rock press resulting from the preliminary fracture of Red Texas Granite.

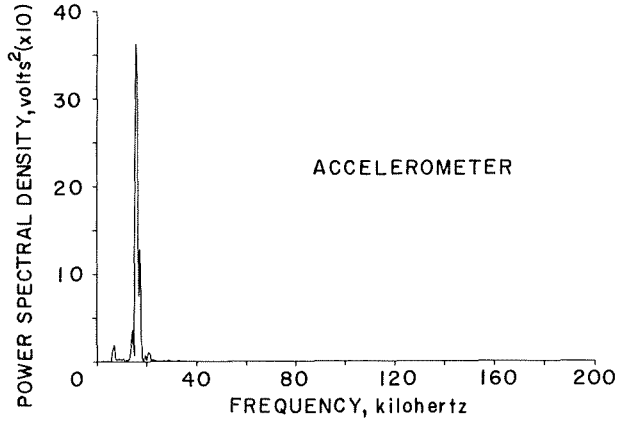

FIGURE 17. - Amplitude spectrum of the accelerometer. Energy is sharply peaked at the accelerometer's resonant frequency of 16 kilohertz.

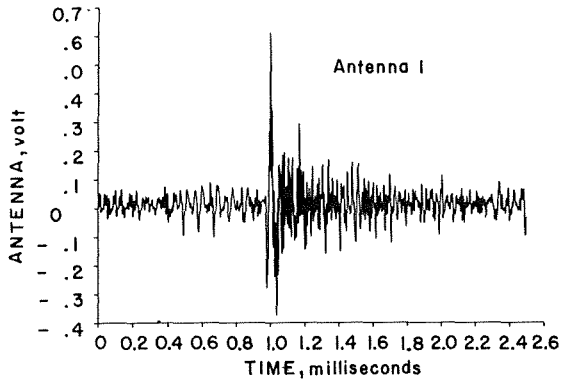

FIGURE 18. - Output of antenna 1, Red Texas Granite sample. Response begins at 0.96 millisecond and attains a maximum peak-to-peak amplitude of 0.99 volt.

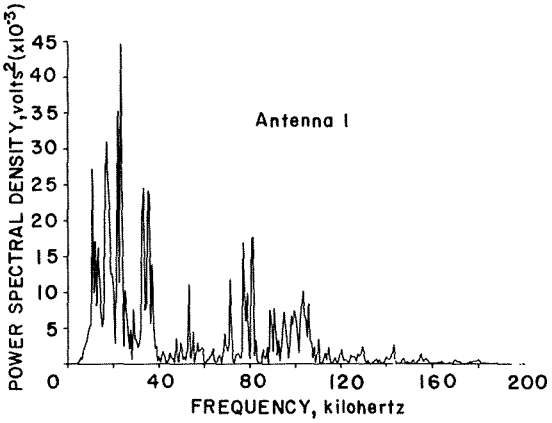

FIGURE 19. - Amplitude spectra of antenna 1 output. The spectrum is more scattered than those for Galena Quartzite, but the majority of energy is still concentrated below 40 kilohertz. Major peaks occur at 10, 17, 22, 23, 33, and 35 kilohertz.

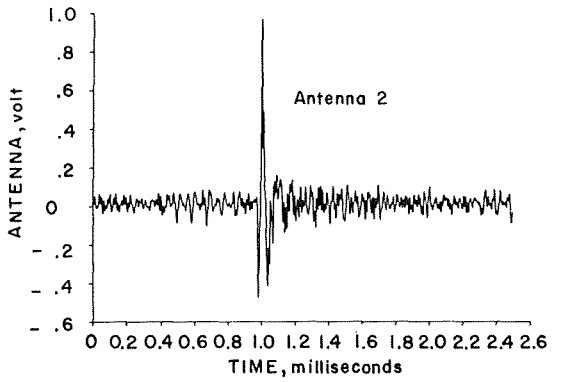

FIGURE 20. - Response of antenna 2 to a preliminary fracture of Red Texas Granite. Maximum amplitude is 1.4 volt, and response begins at 0.96 millisecond.

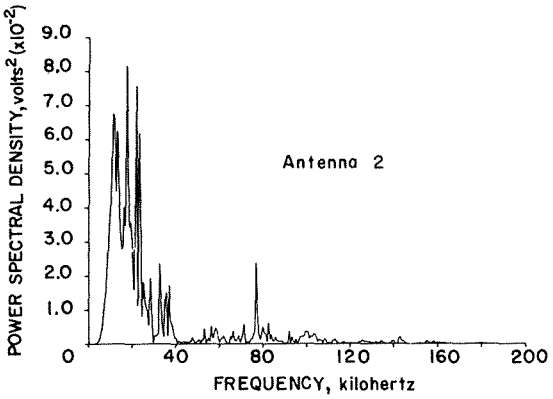

FIGURE 21. - Spectrum of figure 20. Energy lies almost exclusively below 40 kilohertz.

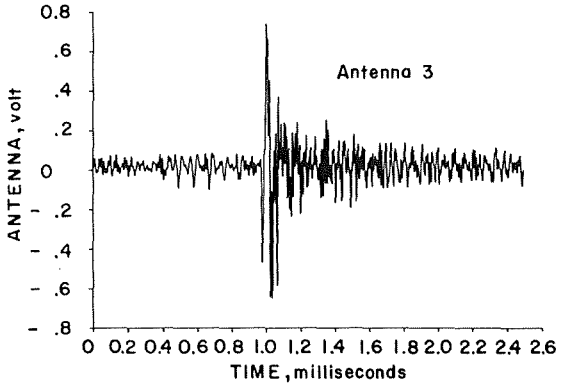

FIGURE 22. - Antenna 3 output showing inception of impulsive event at 0.96 millisecond. Maximum peak-to-peak amplitude is approximately 1.4 volt.

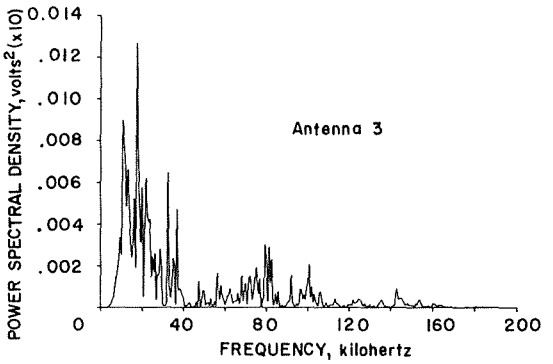

FIGURE 23. - Spectrum of antenna 3, Red Texas Granite. Roughly the same behavior is observed as in figures 24 and 26. Peaks in the spectra occur at 11, 18, and 33 kilohertz.

Barre Granite

Barre Granite is a light-colored, medium-grained, biotite granite. It differs from Red Texas Granite in grain size and ultimate strength. Figure 24 shows the axial load at final failure for a Barre Granite sample. It shows a series of at least six distinct failure events separated by intervals of load stabilization. This contrasts with a smoother, more gradual load drop associated with the failure of the coarser grained Red Texas Granite. Very large antenna responses result from the failure of this specimen (figs. 25-27). All three antennas overdrove the system because the EM emission was of a much higher amplitude than expected. Again in this test, some of the individual failure events on the load can be correlated with EM bursts, and the amplitude of these bursts varies between antennas.

Mather Iron Ore

A powder X-ray diffraction analysis was performed on a sample of iron ore from the Mather A Mine in the Marquette district of Michigan by Dr. E. Booy of the Colorado School of Mines Geology Department. It was learned that this fine-grained, rust-colored taconite was composed mainly of quartz with minor amounts of magnetite, illite, and kaolinite, and trace amounts of hematite. This is a rock type different from those tested previously, but the behavior observed in figures 28 to 30 is essentially the same. Brittle failure of the sample (as seen in the sudden load drop of figure 28) is accompanied by violent changes in both moments (not shown), excitation of the AET (fig. 29) and short bursts of electromagnetic radiation (fig. 30). In this test, all three antennas had about the same amplitude response.

Dakota Sandstone

Dakota Sandstone is a fine- to medium-grained, light-colored sandstone with a quartz cement which will support an ultimate load of only 180 kilonewtons (ultimate stress = 75 megapascals). This is a much lower strength material than those described earlier and deforms nearly plastically. That is, there is really no large sudden load drop that could be associated with a distinct moment of failure. Failure of this rock (and the Carthage Marble described later) seems to take place more by plastic deformation and a loosening of grains than by brittle rupture and its associated sudden load drops.

Although all other devices showed at least some indication of failure, none of the antennas showed any EM response above the ambient noise. This may be because of the more random orientation of the electrical axes of the quartz grains, because no individual failure event released enough energy of itself to initiate a response from the antennas, or because any RF energy released lay outside the bandpass of equipment and so was not detected.

Carthage Marble

This is another relatively soft rock which does not have a sudden catastrophic failure, but rather undergoes a gradual plastic type of deformation. As with Dakota Sandstone, none of the antennas showed any indication of an EM

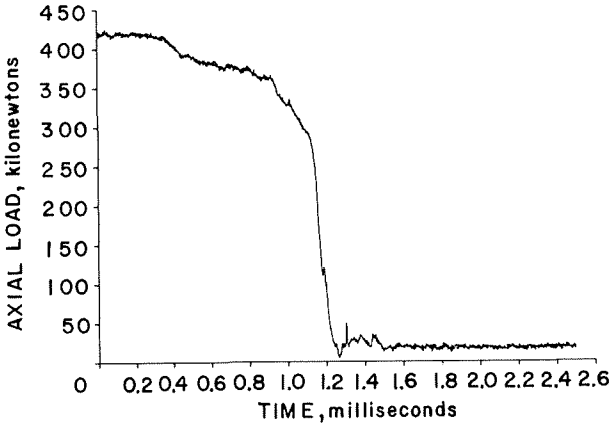

FIGURE 24. - Axial load of Barre Granite at final failure. For this sample, at least five distinct failure events may be seen before final failure at 1.10 milliseconds.

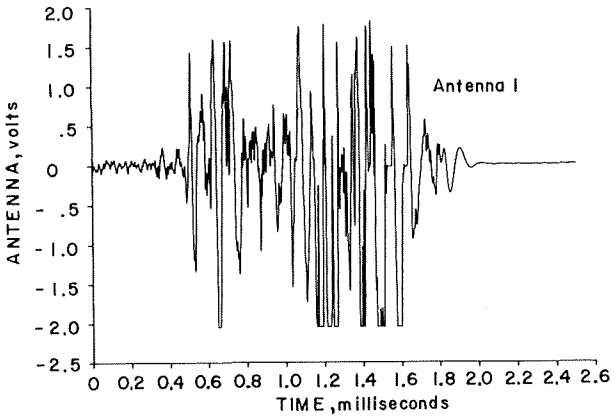

FIGURE 25. - Response of antenna 1 to the failure of Barre Granite. Response begins with the first of the failures shown in figure 24 and continues to form the complex waveform shown.

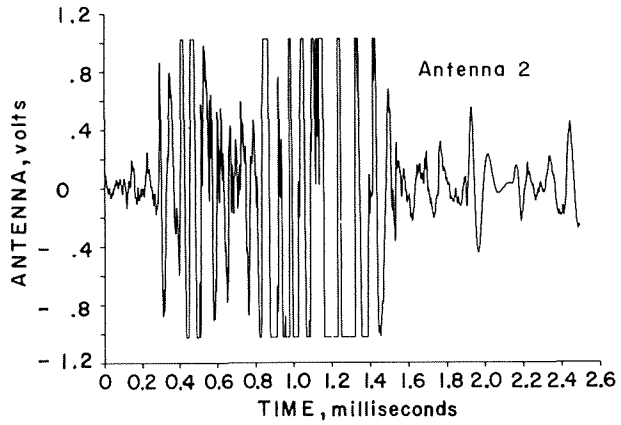

FIGURE 26. - Antenna 2 output from Barre Granite failure. Note that the amplitude scale of figure 25 is twice that of figure 26.

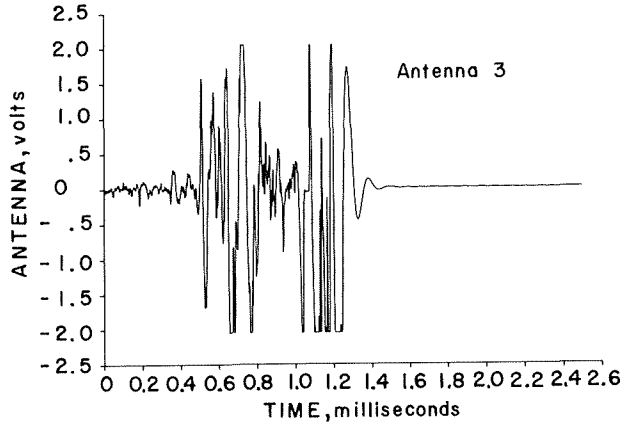

FIGURE 27. - Output of antenna 3. After 1.4 milliseconds the amplifier and filter system of antenna 3 became overdriven.

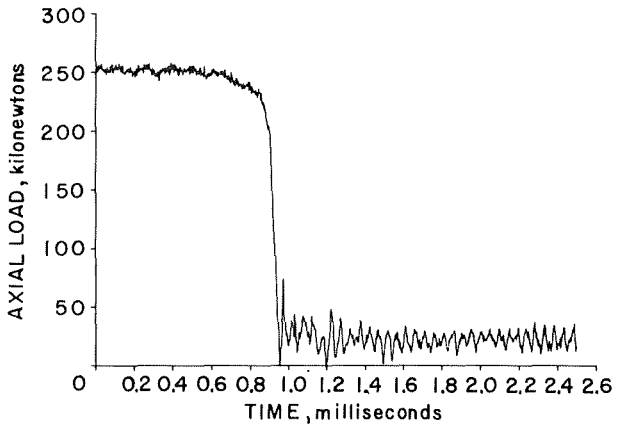

FIGURE 28. - Axial load on Mather Iron Ore at the point of its final failure. The very abrupt drop in load is indicative of a fine-grained, brittle material.

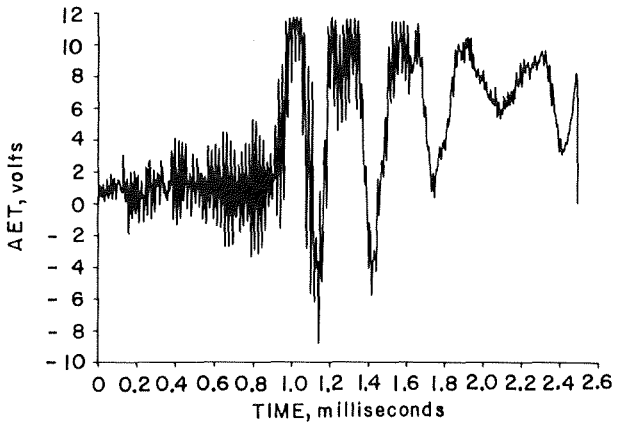

FIGURE 29. - AET signal corresponding to the event shown in figure 28. The AET begins responding as early as 0.1 millisecond and continues ringing throughout the remainder of the trace.

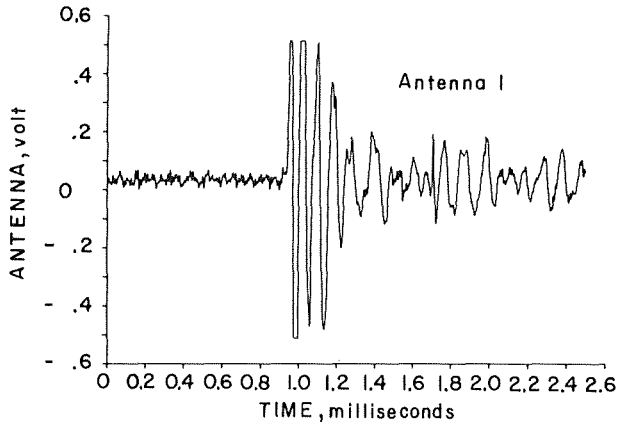

FIGURE 30. - Impulsive response of antenna 1 to the failure of Mather Iron Ore. Inception of this event is slightly later in time than that indicated in figure 28, probably due to mislocation of the event within the sample.

response, while other devices (moment, accelerometer) indicated that failure had indeed occurred. This could be because of a simple lack of generation of any electromagnetic energy for this rock in the bandpass measured, or because stress drops of individual events were too gradual to generate enough energy to produce radiation of a high enough amplitude to be detected, despite the rock's containing piezoelectric minerals.

DISCUSSION

Major Results

Analysis of the data collected leads to five major observations:

1. The formation of failure zones within certain rocks is accompanied by bursts of electromagnetic radiation.

2. Where radiation is observed, its energy is concentrated below 40 kilohertz and there is almost no energy between 40 kilohertz and 160 kilohertz regardless of rock type or grain size.

3. Amplitudes of the emission of this radiation present indications of its being directional.

4. Emission was seen for all quartz-bearing rocks except sandstone. A nonpiezoelectric marble was tested, and no emission was detected.

5. It was observed, in agreement with Nitsan (15), that the amplitude of emission seemed to be independent of stress; however, it did not seem to be independent of stress drop. Larger stress drops for individual events is a measure of crack size and energy released. It has been observed that as these stress drops increase in amplitude, the amplitude of the EM emission also increases.

Nitsan (15) observed emission in the range of 1 to 10 megahertz using a 40 decibel amplifier with a bandwidth of 0.1 to 400 megahertz. In this frequency range his system had a nearly flat frequency response. In the work performed here, the frequency band was lowered to 10 to 400 kilohertz, and a much different spectral response was observed (figs. 8, 10, 12, 19, 21, and 23). The difference between the peaked emissions seen in this work and Nitsan's "white" spectrum can possibly be explained in two ways. The first is that two regions of emission occur, the first below 40 kilohertz and the second above 1 megahertz. The second is that there is but one band of major emission, below 40 kilohertz. Radiation most probably occurs over the entire spectrum but at a lower energy level than that seen between 10 and 40 kilohertz.

An additional result of this work is the interpretation of amplitude variations as being indicative of directionality or the creation by multiple sources of nodal planes in the near or quasi-static electromagnetic field. The apparent directionality indicates that the crack cannot be viewed as a simple isotropic radiator of electromagnetic energy. If this directionality

exists, there must be a focusing mechanism active, be it simply the creation of interference patterns as with parasitic antenna arrays, or some other mechanism which creates "beams" of electromagnetic energy.

Emission Models

In 1977 Nitsan (15) put forward the hypothesis that the rapid decay of the piezoelectric field with the stress drop accompanying fracture was the most probable mechanism of emission. He quoted figures for field gradients of 10^8 volts per meter at the failure point of quartz and charge displacements of 10^{-7} coulomb affected volume of 1 cubic centimeter. He then proposed that emission was related to the rate at which the stress was released and so was inversely proportional to the grain size.

Experimental work performed here supports some points of Nitsan's hypothesis and creates problems for others. The presence of piezoelectric minerals is definitely a criterion for RF emission, but just how emission is related to the creation of intense piezoelectric fields is still not completely understood. Rock types tested in this paper ranged from very coarse-grained Red Texas Granite to very fine-grained Galena Quartzite and Mather iron ore. In the lower frequency range examined, no significant variation in power spectra with grain size can be observed. This seems to indicate that whatever mechanism is responsible for emission, it is more dependent on the generation of intense fields than on the size of the grains broken. It is possible that different mechanisms are responsible for emission in the two different frequency bands investigated (by Nitsan and the Bureau of Mines).

A slightly different hypothesis from Nitsan's involves the acceleration of exoelectrons freed by the formation of a failure zone (8-10). Nitsan reported that the piezoelectric field of a quartz crystal under local stress can reach values of 10^8 volts per meter (15). Any charged particle freed by failure will be accelerated by this field and will radiate energy as it is captured by nearby ions or is otherwise decelerated (12). If the piezoelectric fields created in the stressed rock have a much greater gradient in one direction than in any other, confinement of these charged particles into a fairly narrow beam could occur, resulting in a directional radiation pattern (12). If the tip of the growing crack were to reach the surface with its high potential gradient, exoelectrons could be ejected from the surface of the rock with considerable energy. This fits the observation of exoelectrons with as high an energy as 100,000 electronvolts (10). In rocks that do not contain piezoelectric minerals, exoelectrons are still produced, but there are no strong fields present to accelerate or confine them and so no RF radiation is observed.

In addition, the piezoelectric field for a rock aggregate will increase only up to a certain saturation level (16). The potential for a quartz-bearing material will only go to a saturation value, no matter how many crystals are fractured at any one time. Assuming that the rate of stress drop is roughly the same for each individual failure event, the saturation limit would seem to limit the magnitude of radiation caused by rapid field decay. If, on the other hand, emission derives a significant portion of its energy from the

acceleration of charged particles, the more electrons freed, the more energy available for radiation. Hence, larger failure zones should generate larger EM signals. This fracture size-radiation amplitude relation has been observed experimentally and so gives weight to the proposal that some mechanism of this nature is in effect. It is possible, however, that in the laboratory experiments performed here, the saturation limit for the piezoelectric effect has not been reached.

All rocks tested in this series of experiments had been stored in the air for at least 2 years and were dry. Thus, the diffusion of water into the failure zone is not a necessary condition for the emission of RF radiation.

It should be stressed that neither of the above mechanisms can be ruled out, nor can one be overwhelmingly favored. It is very possible that both exist and contribute to some portion of the EM radiation observed. Laboratory work has not progressed far enough to select one model to the exclusion of all others.

Finally, it seems rather coincidental that sferics (naturally occurring fluctuations of the atmospheric electromagnetic field) reported to have accompanied earthquakes (7) should have frequencies of 10 to 20 kilohertz, nearly the same frequencies as the major portion of the electromagnetic energy observed to be emitted by rock failure in this study. From this, it seems possible that these sferics are the product of the larger scale failure of rocks during earthquakes.

Applications

The most important application for electromagnetic emissions observation is the monitoring of unstable rock faces in mines or possibly monitoring activity along faults. In mining applications a portable system could be devised since the antenna need not be coupled directly to the rock face as with conventional geophones. An increase in the number or amplitude of events could signal an impending rock burst.

This system seems practical on a mine scale for two reasons. First, if, as implied in this study, the amplitude of emission increases with crack size, mine-type failures could produce significant signals. Second, calculations of skin depth for dry rock indicate a depth of penetration of the signal which is practical for mine scale applications. As calculated before, the skin depth at 20 kilohertz is on the order of 1,000 meters. Saturating fluids will reduce this value, but to what extent is unknown.

A series of field experiments is planned to test the applicability of this system in the Galena Mine, Wallace, Idaho.

CONCLUSIONS

Fracture in rock materials containing piezoelectric minerals was shown to be accompanied by the emission of bursts of radiofrequency electromagnetic energy. Detection of these bursts is a fairly simple operation, requiring only a dipole antenna with filters and amplifiers appropriate to the frequency band to be investigated.

These RF signals were observed in the range of 10 to 200 kilohertz. With the results of Nitsan (15), the known frequency range of emission extends from roughly 10 kilohertz to 10 megahertz, although it is very possible that emission extends into lower and higher frequencies. Power spectra of antenna signals show their energy to be sharply peaked between 10 and 40 kilohertz.

The RF emission observed had two other characteristics. It increased in amplitude with increasing event size, and it exhibited an apparent directionality. As the amplitude of acceleration and acoustic emission increased, so did the amplitude of RF emission. An array of three monopole antennas placed around the sample tested showed amplitude variations for the same event of as much as 4:1, which were interpreted as directionality in emission.

While emission was seen only for rocks containing piezoelectric minerals, just what the relation between piezoelectric fields and emission is, is not fully understood. Proposed mechanisms of emission include the rapid drop in piezoelectric field with fracture of the crystal and/or the acceleration of freed exoelectrons by the very intense local piezoelectric field gradients.

The application of EM radiation to monitor slope and rock wall instabilities appears promising, as larger events cause larger signals and in the 20 kilohertz range, dry rock is fairly transparent. On a still larger scale, depending on rock and failure type, it may become feasible to monitor faults for activity and rupture propagation direction by using arrays of antennas.

REFERENCES

1. Booker, J. R. Dilatancy and Crustal Uplift. Pure and Applied Geophysics, v. 113, 1975, pp. 119-125.

2. Brady, B. T. Theory of Earthquakes, Part I: A Scale Independent Theory of Rock Failure. Pure and Applied Geophysics, v. 112, 1975, pp. 701-725.

3. _____. Theory of Earthquakes, Part II: Inclusion Theory of Crustal Earthquakes. Pure and Applied Geophysics, v. 113, 1975, pp. 149-168.

4. _____. Theory of Earthquakes, Part III: Inclusion Collapse Theory of Deep Earthquakes. Pure and Applied Geophysics, v. 114, 1976, pp. 119-139.

5. _____. Theory of Earthquakes, Part IV: General Implications for Earthquake Prediction. Pure and Applied Geophysics, v. 114, 1976, pp. 1031-1082.

6. Cherry, J. T., R. N. Schock, and J. A. Sweet. A Theoretical Model of the Dilatant Behavior of a Brittle Rock. Pure and Applied Geophysics, v. 113, 1975, pp. 197-206.

7. Derr, J. S. Earthquake Lights: A Review of Observations and Present Theories. Bull. Seismological Soc. America, v. 63, 1963, pp. 2177-2187.

8. Good, R. H., and T. J. Nelson. Classical Theory of Electric and Magnetic Fields. Academic Press, New York, 1971, 636 pp.

9. Hoenig, S. A. Monitoring the Ball-Milling Process by Means of Exoelectron Emission, Mining Cong. J., v. 58, 1972, pp. 34-35.

10. _____. Monitoring Failure Processes in Ceramic Materials by Means of Exoelectron Emission, NSF Rept., 1979, 8 pp.

11. Keller, G. V., and F. C. Frischnecht. Electrical Methods in Geophysical Prospecting. Pergamon Press, New York, 1966, 517 pp.

12. King, R. W. P., and C. W. Harrison, Jr. Antennas and Waves: A Modern Approach, MIT Press, Cambridge, Mass., 1969.

13. Kraichman, M. B. Handbook of Electromagnetic Propagation in Conducting Media. Headquarters Naval Material Command, 1976, 109 pp.

14. Mjachkin, V. I., W. F. Brace, G. A. Sobolev, and J. H. Dieterich. Two Models of Earthquake Forerunners. Pure and Applied Geophysics, v. 113, 1975, pp. 169-181.

15. Nitsan, U. Electromagnetic Emission Accompanying Fracture of Quartz-Bearing Rocks. Geophysical Research Letters, v. 4, 1977, pp. 333-336.

16. Parkhomenko, E. I. Electrification Phenomena in Rocks. Plenum Press, New York, 1971, 285 pp.

17. Vorobev, A. A., V. M. Chavsov, and V. F. Gordeev. Pulsed RF Radiation Produced by Scratching Some Dielectrics. Soviet Phys. J., v. 10, 1977, pp. 126-128.

☆U.S. GOVERNMENT PRINTING OFFICE: 1981-505-002/107 INT.-BU.OF MINES,PGH.,PA. 25680